www.elsevier.com/locate/jcrysgro

Growth and characterisation of sulphur-rich $TlIn(S_{1-x}Se_x)_2$ single crystals

A.V. Gomonnai, I. Petryshynets, Yu.M. Azhniuk, O.O. Gomonnai, I.Yu. Roman, I.I. Turok, A.M. Solomon, R.R. Rosul, D.R.T. Zahn

PII: S0022-0248(13)00045-6
DOI: http://dx.doi.org/10.1016/j.jcrysgro.2013.01.008
Reference: CRYS21372

To appear in: *Journal of Crystal Growth*

Received date: 4 May 2012
Revised date: 12 December 2012
Accepted date: 5 January 2013

Cite this article as: A.V. Gomonnai, I. Petryshynets, Yu.M. Azhniuk, O.O. Gomonnai, I.Yu. Roman, I.I. Turok, A.M. Solomon, R.R. Rosul and D.R.T. Zahn, Growth and characterisation of sulphur-rich $TlIn(S_{1-x}Se_x)_2$ single crystals, *Journal of Crystal Growth,* http://dx.doi.org/10.1016/j.jcrysgro.2013.01.008

Growth and characterisation of sulphur-rich $TlIn(S_{1-x}Se_x)_2$ single crystals

A.V. Gomonnai[1], I. Petryshynets[2], Yu.M. Azhniuk[1], O.O. Gomonnai[3], I.Yu.Roman[1], I.I.Turok[1], A.M.Solomon[1], R.R.Rosul[3], D. R. T. Zahn[4]

[1] Institute of Electron Physics, Ukr. Nat. Acad. Sci., Universytetska Str. 21, 88017 Uzhhorod, Ukraine, e-mail: gomonnai@ukr.net

[2] Institute of Materials Science, Slovak Academy of Sciences, Watsonova 47, 04001 Košice, Slovakia

[3] Uzhhorod National University, Pidhirna Str. 46, 88000 Uzhhorod, Ukraine

[4] Semiconductor Physics, Chemnitz University of Technology, Reichenhainer Str. 70, D-09107 Chemnitz, Germany

Abstract.

Sulphur-rich $TlIn(S_{1-x}Se_x)_2$ single crystals ($0 \le x \le 0.10$) were grown by the Bridgman technique. Their structure and composition are studied by X-ray diffraction, scanning electron microscopy, energy-dispersive X-ray spectroscopy, and Raman scattering. In the Raman spectra, besides the typical one-mode and two-mode features, bands corresponding to internal vibrations of "mixed" $In_4S_{10-y}Se_y$ structural groups are revealed.

Keywords:

A1. X-ray diffraction, A2. Bridgman technique, A2. Single crystal growth, B2. Ferroelectric materials.

1. Introduction

$TlInS_2$ and $TlInSe_2$ single crystals possess highly anisotropic (layered and chain-like, respectively) structure and with decreasing temperature they reveal a series of phase transitions, including those to incommensurate and ferroelectric phases [1–4]. Their structure has been subject of extensive studies not only due to complex structural transformations with temperature and pressure [1–17], but also in view of possible applications in optoelectronics due to their high photosensitivity in the visible spectral range, high birefringence, and broad transparency range [18] as well as photoinduced phenomena enabling memory effects [19] and promising thermoelectric properties [20]. Anionic substitution provides an additional means of variation of structural transformation temperatures which in other chalcogenide ferroelectric systems is known to result in multicritical points [21, 22]. Quite a few studies using Raman scattering [23], infrared reflection spectra [24, 25], and dielectric measurements [26, 27] of the mixed crystals of $TlIn(S_{1-x}Se_x)_2$ system were reported. As follows from the data available, at Se concentration of about 0.7–0.75 the crystal structure changes from C_{2h}^6 to D_{4h}^{18} [23, 26]. Most of the studies were performed for series of samples with a rather limited number of compositions within the whole x interval. Only in Refs. 26 and 27 particular attention was paid to sulphur-rich $TlIn(S_{1-x}Se_x)_2$ single crystals with $x < 0.2$. Based on the dielectric measurements, S→Se substitution in $TlIn(S_{1-x}Se_x)_2$ crystals was shown to result in a decrease of the phase transition temperatures and a simultaneous narrowing of the incommensurate phase interval, leading to a Lifshitz-type polycritical point at $x = 0.05$ [27]. Note that several studies were devoted to solid solutions of related $TlIn_{1-x}Ga_xS_2$ [28–30] and $TlIn_{1-x}Ga_x(S_{1-x}Se_x)_2$ [31] systems.

Here we report on the growth of sulphur-rich $TlIn(S_{1-x}Se_x)_2$ solid solution single crystals and their characterisation by X-ray diffraction,

scanning electron microscopy, energy-dispersive X-ray spectroscopy, and Raman scattering.

2. Experimental

The initial mixture for $TlIn(S_{1-x}Se_x)_2$ compounds was prepared from high purity elemental substances loaded in required proportions into quartz ampoules which were evacuated down to 1.3×10^{-2} Pa and sealed. The synthesis was carried out by local heating in the flame of an oxyfuel burner. This method enables to observe the synthesis process visually, to control the temperature and the interaction rate and makes the process faster by an order of magnitude. The same ampoules were used for growth, their shape being shown in Fig. 1. Performing the synthesis and growth in the same ampoules enabled us to avoid reloading of the synthesised mixture, reducing the probability of its additional contamination. After the synthesis, the melt was crystallized by cooling down to room temperature in the horizontally oriented ampoules what enabled a better filling of the ampoule and prevented the subsequent ampoule cracking when it was afterwards vertically loaded into the oven.

The temperature profile of the oven hot zone (See Fig. 1) was chosen in assumption that the whole mixture in the growth ampoule was in the molten state above the crystallisation point. A slight increment of temperature in the upper part of the melt zone enabled us to prevent partial condensation of volatile components of the melt in the upper part of the ampoule. The position of the crystallisation point in the oven was determined by calibration of the vertical profile using chromel–alumel and platinum–(platinum+rhodium) thermocouples. Since the ampoule with the melt introduces some anomalies in the temperature distribution in the crystallisation zone due to thermal conductivity, the position of the boundary between the solid phase and the melt in the ampoule beak was visually controlled by taking the ampoule out of the oven operating volume for a short time (2–3 s) and correction of its

depth position. During this procedure the boundary between the melt and the solid phase could be well observed due to the presence of gas bubbles at the ampoule walls in the molten phase. In the course of crystallization the gas bubbles were driven further into the melt by the crystallization front. By subsequent stagewise annealing and augmentation of the solid phase in the beak for nucleation a single crystal seed was formed. $TlIn(S_{1-x}Se_x)_2$ single crystals were grown by the Bridgman technique. The crystallisation front speed after the seeding was 0.25–0.28 mm/h, the temperature gradient in the crystallization zone 2.0–3.5 °C/min, the temperature stability ±0.3 °C, the melt zone temperature (850±10) °C, the "cold" zone temperature (550±20) °C, cooling rate after the growth 30–50 °C/h.

For X-ray diffraction (XRD) studies single crystals were reground to fine powder in an agate mortar. X-ray powder diffraction studies were carried out at room temperature using a conventional Bragg–Brentano technique with a DRON-4 diffractometer and Cu K_α radiation. Besides, diffractograms of cleaved surfaces of $TlIn(S_{1-x}Se_x)_2$ single crystals were measured.

Scanning electron microscopy (SEM) studies combined with energy dispersive X-ray spectroscopy (EDX) were performed using a SEM JEOL 7000F microscope.

Micro-Raman measurements were performed in a Z(XX+XY)Z backscattering configuration using a Horiba LabRAM HR spectrometer with diffraction gratings of 2400 slits/mm and a CCD camera. An Ar^+ laser operating at 514.5 nm was used for excitation. The measurements were carried out at room temperature.

3. Results and discussion

Using the above described technique enabled us to obtain $TlIn(S_{1-x}Se_x)_2$ ($0 \le x \le 0.1$) single crystals shown in Fig. 2. In most cases the axis of the crystal growth was within the (001) cleavage plane, in some cases the angle between this plane and the growth axis was 40–50°. In our opinion, it is quite probable that the orientation of the cleavage plane is strongly determined by the position of the crystallisation point at the gradient section of the temperature profile of the oven (See Fig. 1).

Powder X-ray diffraction data for the grown $TlIn(S_{1-x}Se_x)_2$ single crystals are illustrated by Fig. 3. It is known that $TlInS_2$ can crystallize in monoclinic, triclinic, tetragonal, orthorombic, and hexagonal crystal systems, in most cases forming layered (monoclinic and triclinic) or layered-and-chainlike (orthorombic and hexagonal) structures [32–35]. Moreover, different polytypes of monoclinic and possibly triclinic $TlInS_2$ crystals can exist [34]. The ample variety of possible structures makes the XRD analysis a non-trivial task, especially in view of the close values of the XRD peak positions reported for different structures. The measured diffraction patterns of the $TlInS_2$ crystal (the lowest curve in Fig. 3) reveal clear peaks, the positions of which are in good agreement with the available data for the C_{2h}^6 space group (monoclinic structure) most often reported for the structure stable at room temperature and atmospheric pressure [33]. Some weaker features could result from the presence of more complicated polytypes. The X-ray diffraction pattern measured from the single crystal cleaved surface (Fig. 4) appears similar to the one obtained from the powder.

With partial S→Se substitution in the single crystals the XRD patterns remain basically similar. Only a slight gradual shift of the diffraction peak positions with increasing sulphur content in the mixed crystals is observed for

both powders and $TlIn(S_{1-x}Se_x)_2$ single crystals, clearly seen for the highest XRD peak (initial peak position $2\theta = (23.91\pm0.04)°$ for $TlInS_2$) from the insets in Figs. 3 and 4, respectively. For the $TlIn(S_{0.9}Se_{0.1})_2$ crystal, the position of corresponding peak in the insets shifts down to $(23.75\pm0.04)°$, indicating a slight increase of the lattice parameter by up to 1 %. From the measured XRD data one can conclude that the grown sulphur-rich $TlIn(S_{1-x}Se_x)_2$ single crystals belong to the same structural group with a smooth compositional variation of the lattice parameter.

A typical SEM pattern of the cleaved surface of a $TlIn(S_{1-x}Se_x)_2$ single crystal is shown in Fig. 5. Our SEM data did not enable us to observe misorientation of layers which is a well known structural defect of this family [29, 40]. SEM measurements were performed for the crystals with different composition, combined with EDX analysis, the EDX spectra being shown in Fig. 6.

As follows from the EDX data, the presence of thallium, indium, and sulphur is confirmed for all crystals under investigation. For the single crystals with selenium content $x \geq 0.03$ the presence of selenium is also clearly confirmed. The quantitative estimation of the content of the corresponding elements correlates with their concentration in the initial mixture. However, as can be seen from Fig. 6, practically in all cases the ratio of compositions of indium and thallium is above unity, showing an overestimation of In and/or underestimation of Tl concentration. Evidently, this should be the result of some calibration error with regard to Tl and In content evaluation, and in this case our EDX data cannot be considered ultimate for the quantitative determination of the elemental composition unless the appropriate calibration procedures are made. Still, the EDX-based sulphur-to-selenium ratio values are quite reasonable and correlate well with the content of chalcogens in the initial mixture. The corresponding correlation is seen from Fig. 7.

Room-temperature Raman spectra of $TlInS_2$ crystal were studied quite extensively [5, 7, 8, 36–41]. As noted above, different structures and polytypes of this crystal are known to exist, the most typical and extensively studied being the structures described by C_{2h}^6 [7, 8, 41] and D_{4h}^{18} [7] space groups. It is the chain-like tetragonal structure with D_{4h}^{18} symmetry group that is reported for the room-temperature $TlInSe_2$ crystal phase [42], Raman studies of which are also quite extensive [38, 43–45]. Group-theoretical predictions for the Raman-active vibrations in $TlInS_2$ were the subject of detailed analysis [7, 8, 41]. The most recent data predict for the monoclinic C_{2h}^6 room-temperature phase the existence of $10A_g + 14B_g$ Raman-active modes [41]. For tetragonal (D_{4h}^{18}) $TlInSe_2$ crystal the analysis predicts $1A_{1g} + 2A_{2g} + 2B_{2g} + 3E_g$ zone-center modes [38, 44].

The experimentally measured Raman spectra of $TlIn(S_{1-x}Se_x)_2$ single crystals are shown in Fig. 8. Since, as follows from the above XRD data, the sulphur-rich $TlIn(S_{1-x}Se_x)_2$ crystals, are isostructural to $TlInS_2$, one should expect in the Z(XX+XY)Z configuration the vibrations of A_g symmetry to be revealed. The Raman peaks at 48, 62, 80, 137, 280, 291, and 345 cm^{-1} in the figure for $TlInSe_2$, agree with the known data for the A_g vibrations [7, 8, 40, 41]. Besides, a weak maximum at 97 cm^{-1} evidently corresponds to the forbidden B_g mode which is known to be quite intense in the allowed geometry [7]. The lower-frequency bands at 19 and 37 cm^{-1} reported earlier [7, 8] were beyond the spectral range under investigation while the known A_g bands at 43 and 115 cm^{-1} [7] were not resolved due to their weakness, the first of them actually being slightly revealed as a shoulder of the band with the peak at 48 cm^{-1} while the weak band at 115 cm^{-1} [7] was not observed by other authors either [8, 40]. As follows from the literature, the higher-frequency bands are related to the "intramolecular" vibrations of more rigid In_4S_{10} tetrahedral structural groups which are known to be bonded by ionic-

covalent bonds with Tl atoms located in the voids between them [40]. Meanwhile, lower-frequency bands correspond to translational vibrations governed by weaker interactions of van-der-Waals type for the bonds between the In_4S_{10} tetrahedra and ionic forces binding Tl^+ to InS_2^- ions [40].

As one could expect, with partial substitution of sulphur by selenium, practically no changes were revealed in the low-frequency part of the Raman spectrum of $TlIn(S_{1-x}Se_x)_2$ crystals. A slight downward shift of the intermediate frequency band from 137 to 135 cm^{-1} is in agreement with the one-mode compositional behaviour [23, 24] which is typical for vibrations external with respect to pronounced structural groups (in this case, the In_4S_{10} tetrahedra).

Meanwhile, in the higher-frequency range one can observe new bands to appear near 200 cm^{-1} already at a selenium concentration as low as 1 %. With increasing *x*, the two bands at 198 and 205 cm^{-1} are better resolved and grow in intensity. Their frequency positions remain practically unchanged, exhibiting a very slight trend to decrease with *x*. Simultaneously, a similar tiny decrease is observed for the frequency positions of the high-energy bands at 280, 291, and 345 cm^{-1} corresponding to the "intramolecular" vibrations of the In_4S_{10} tetrahedra. The comparison of the intensities of the sulphide-like bands slightly below 300 cm^{-1} and the observed bands near 200 cm^{-1} evidently related to the S→Se substitution in the Raman spectra of $TlIn(S_{1-x}Se_x)_2$ crystals shows a good correlation with the crystal composition in the interval under investigation (Fig. 9).

At a first glance, these should be typical signatures for the two-mode behaviour which is, as a rule, observed for the vibrations of pronounced structural groups in compounds with large number of atoms in the unit cell. Hence, this should mean that the new bands arising in the spectra of $TlIn(S_{1-x}Se_x)_2$ crystals near 200 cm^{-1} correspond to the vibrations of structural groups of In_4Se_{10} type tetrahedra similar to those at 280 and 291 cm^{-1} in $TlInS_2$. As

one can see from the $TlInSe_2$ Raman spectrum measured in the same experimental configuration (Fig. 10), for this compound similar intense peaks are located at 171 and 183 cm^{-1}. Even though the observed compositional trend seems to be in at least qualitative agreement with what is predicted by the two-mode behaviour, quantitatively one should expect a noticeably stronger compositional shift of the phonon frequencies. Besides, the observed phonon frequencies contradict the Raman and infrared data for the selenide-like phonons in mixed crystals with higher Se content [23, 24].

However, it should be mentioned that if the crystal structure contains several atoms of one sort in a pronounced structural group, in mixed crystals, due to partial isovalent substitution, not only the end-point structural groups (in this case, In_4S_{10} and In_4Se_{10} tetrahedra) can be present in the structure, but also more complicated units with different number of substitutive atoms (in this case, $In_4S_{10-y}Se_y$ with y from 1 to 9). For small concentrations of one of the atomic species (in our case, selenium) there is no physical reason to expect that tetrahedra where S is completely substituted by Se will be predominant in the solid solution structure. Moreover, from the mere comparison of probabilities for such small x it is much more likely to expect mixed $In_4S_{10-y}Se_y$ groups to dominate over the In_4Se_{10} tetrahedra.

For different solid solution systems, the existence of mixed structural groups of similar type was confirmed by Raman spectroscopy where they are characterized by bands whose frequencies are between the corresponding vibration frequencies for the end-point groups (*e. g.* [46]). Earlier Raman studies of $TlIn(S_{1-x}Se_x)_2$ solid solutions with higher Se content [23] reported a maximum revealed near 200 cm^{-1} for the crystals with x ranging from 0.4 to 0.6 which was attributed to sulphur-selenium vibrations. It is this frequency range where we observe quite distinct maxima near 197 and 205 cm^{-1} for the samples with x below 0.1. Hence, it is reasonable to assume that the two bands in question are related to the vibrations of S and Se atoms in the

"mixed" $In_4S_{10-y}Se_y$ tetrahedra. Moreover, for $x \geq 0.05$ one can clearly observe a weak though quite distinct Raman band near 173 cm^{-1} which is evidently related to the vibrations of the In_4Se_{10} tetrahedra.

The observed features of one-mode and two-mode behaviour as well as the identified vibrations of "mixed" $In_4S_{10-y}Se_y$ structural groups in $TlIn(S_{1-x}Se_x)_2$ crystals are in reasonable agreement with the Raman data for the compositional transformation of the phonon spectra in other solid solution systems of this family, reported earlier for $TlGa(S_{1-x}Se_x)_2$ [23, 40] and $TlGa_{1-x}In_xS_2$ [29, 40]. The model proposed in Ref. 40 can be applied to evaluate the compositional shifts of the phonon frequencies. However, due to the small content of selenium, the compositional shifts were too small. Even for the highest Se content $x = 0.1$ the most pronounced frequency shifts for the $TlInS_2$-like bands from 280 to 278 cm^{-1} and from 291 to 290 cm^{-1} were just comparable or even below the discrepancies in the frequency values for $TlInS_2$ obtained by different authors [8, 9, 38, 40, 42]. Evidently, the model of Ref. 40 should be used for a broader set of compositions with more extensive polarization measurements to be performed in the nearest future.

Conclusions

Sulphur-rich $TlIn(S_{1-x}Se_x)_2$ single crystals with $0 \leq x \leq 0.10$ were grown by the Bridgman technique. The X-ray diffraction studies performed for powders as well as cleaved surfaces confirm the similarity of their structure at room temperature to that of $TlInS_2$ with a slight variation of the lattice parameter with S→Se substitution. SEM+EDX studies confirm the uniformity of the crystal composition over the surface and show a good correlation with the chalcogen concentration in the initial mixture. Raman spectra of the sulphur-rich $TlIn(S_{1-x}Se_x)_2$ single crystals show a one-mode type behaviour for lower-frequency translational and librational vibrations external with respect to the pronounced $In_4[S(Se)]_{10}$ structural groups. Meanwhile, for the higher-frequency internal vibrations of these groups, in the compositional

interval under investigation, features typical for the two-mode behaviour in solid solutions are revealed with a slight compositional shift of the band frequencies and appearance of bands corresponding to vibrations of "mixed" $In_4S_{10-y}Se_y$ structural groups rather than those of In_4Se_{10} tetrahedra. This is evidently related to the quite low selenium concentration.

Acknowledgements

This work was supported by Science and Technology Center in Ukraine (project No. 5208). Yu. M. Azhniuk is grateful to Deutscher Akademischer Austausch Dienst for the support of his Raman measurements at Chemnitz University of Technology.

References

[1] N. A. Abdullaev, K. R. Allakhverdiev, G. L. Belenkii, T. G. Mamedov, R. A. Suleimanov, and Ya. N. Sharifov, Sol. State Commun. 53 (1985) 601–602.

[2] R. Laiho, T. Levola, R.M. Sardarly, K.R. Allakhverdiev, I.Sh. Sadykov, and M.M. Tagiev, Sol. State Commun. 63 (1987) 1189–1192.

[3] K.R. Allakhverdiev, N. Türetken, F.M. Salaev, and F.A. Mikailov, Sol. State Commun. 96 (1995) 827–831.

[4] S. Kashida and Y. Kobayashi, J. Phys.: Condens. Matter 11 (1999) 1027–1035.

[5] W. Henkel, H. D. Hochheimer, C. Carlone, A. Werner, S. Ves, and H. G. v. Schnering, Phys. Rev. B 26 (1982) 3211–3221.

[6] A.D. Belyaev, Yu.P. Gololobov, V.F. Machulin, K.R. Allakhverdiev, and T.G. Mamedov, Ukr. Fiz. Zh. 33 (1988) 582–584 [in Russian].

[7] K.R. Allakhverdiev, S.S. Babaev, N.M. Tagiev, and M.M. Shirinov, Phys. Status Solidi B 152 (1989) 317–327.

[8] V.M. Burlakov, A.P. Ryabov, M.P. Yakheev, E.A. Vinogradov, N.N. Melnik, and N.M. Gasanly, Phys. Status Solidi B 153 (1989) 727–739.

[9] B. Abay, H. S. Güder, H. Efeoğlu, Y. K. Yoğurtçu, J. Appl. Phys. 84 (1998) 3872–3879.

[10] F.A. Mikailov, E. Başaran, T.G. Mammadov, M.Y. Seyidov, and E. Şentürk, Physica B 334 (2003) 13–20.

[11] J. Grigas and E. Talik, Phys. Status Solidi B 237 (2003) 494–499.

[12] A.F. Qasrawi and N.M. Gasanly, Phys. Status Solidi A 199 (2003) 277–283.

[13] Y.G. Shim, N. Uneme, S. Abdullayeva, N. Mamedov, and N. Yamamoto, J. Phys. Chem. Solids 66 (2005) 2116–2118.

[14] A.F. Qasrawi and N.M. Gasanly, J. Mater. Sci. 41 (2006) 3569–3572.

[15] E. Sentürk, L. Tumbek, F. A. Mikailov, and F. Salehli, Cryst. Res. Technol. 42 (2007) 626–630.

[16] O.O. Gomonnai, P.P. Guranich, M.Y. Rigan, I.Y. Roman, and A.G. Slivka, High Pressure Research 28 (2008) 615–619.

[17] A.M. Panich, J. Phys.: Condens. Matter 20 (2008) 293202-1–293202-42.

[18] K.R. Allakhverdiev, Sol. State Commun. 111 (1999) 253–257.

[19] S. Özdemir, R.A. Süleymanov, K.R. Allakhverdiev, F.A. Mikailov, and E. Civan, Sol. State Commun. 96 (1995) 821–826.

[20] N. Mamedov, K. Wakita, A. Ashida, T. Matsui, and K. Morii, Thin Solid Films 499 (2006) 275–278.

[21] A.V.Gomonnai, A.D. Belyaev, V.F. Machulin, N.F. Korda, and V.Yu. Slivka, Fiz. Tverd. Tela 23 (1981) 1623–1625 [in Russian].

[22] A.V.Gomonnai, A.A. Grabar, Yu.M. Vysochanskii, A.D. Belyaev, V.F. Machulin, M.I. Gurzan, and V.Yu. Slivka, Fiz. Tverd. Tela 23

(1981) 3602–3607 [in Russian].

[23] N. A. Bakhyshov, N. M. Gasanly, B. M. Yavadov, V. I. Tagirov and Sh. M. Efendiev, Phys. Status Solidi B 91 (1979) K1–K3.

[24] N.M.Gasanly, B.M.Dzhavadov, V.I.Tagirov, and E.A.Vinogradov, Phys. Status Solidi B 95 (1979) K27–K30.

[25] K.R. Allakhverdiev, N.D. Akhmedzade, N.M. Tagiev, M.M. Shirinov, and S. Häseler, Phys. Status Solidi B 148 (1988) K93–K96.

[26] M.Yu. Seyidov, R.A. Suleymanov, and F. Salehli, Phys. Scripta 84 (2011) 015601-1–015601-7.

[27] M.Yu. Seyidov, R.A. Suleymanov, and F. Salehli, Phys. of the Solid State 51 (2009) 2513–2519.

[28] K.R. Allakhverdiev, N.M. Gasanly and A. Aydinli, Sol. State Commun. 94 (1995) 777–782.

[29] N.M. Gasanly and N.S. Yuksek, Acta Phys. Polon. A 108 (2005) 997–1003.

[30] N.M. Gasanly, Sol. State Commun. 150 (2010) 1656–1659.

[31] K.R. Allakhverdiev, T.G. Mamedov, V.V. Panfilov, E. Yu. Salaev, S.I. Subbotin, and M.M. Shukyurov, Sol. State Commun. 56 (1985) 989–993.

[32] T.J. Isaacs, Z. Kristallogr. B 141 (1971) 104–108.

[33] K.J. Range, G. Engert, W. Müller, and A. Weiss, Z. Naturforsch. B 29 (1974) 181–185.

[34] O. Z. Alekperov and A. I. Nadjafov, Inorg. Mater. 45 (2009) 7–12.

[35] O. Z. Alekperov, G. B. Ibragimov, I. A. Axundov, A. I. Nadjafov, and A. R. Fakix, Phys. Stat. Solidi C 6 (2009) 981–984.

[36] T.J. Isaacs and J.D. Feichter, J. Sol. State Chem. 14 (1975) 260–263.

[37] N.M. Gasanly, B.N. Mavrin, Kh.E. Sterin, V.I. Tagirov, and Z.D. Khalafov, Phys. Status Solidi B 86 (1978) K49–K53.

[38] N.M. Gasanly, A.F. Goncharov, B.M. Dzhavadov, N.N. Melnik, V.I. Tagirov, and E.A. Vinogradov, Phys. Status Solidi B 92 (1979) K139–K142.

[39] K.R. Allakhverdiev, N.Yu. Safarov, M.A. Nizametdinova, E.A. Vinogradov, N.N. Melnik, and S.I. Subbotin, Sol. State Commun. 42 (1982) 485–488.

[40] N.M. Gasanly, A.F. Goncharov, N.N. Melnik, A.S. Ragimov, and V.I. Tagirov, Phys. Status Solidi B 116 (1983) 427–443.

[41] N.S. Yuksek, N.M. Gasanly, and A. Aydinli, J. Raman Spectrosc. 35 (2004) 55–60.

[42] D. G. Kilday, D. W. Niles, G. Margaritondo, and F. Levy, Phys. Rev. B 35 (1987) 660–663.

[43] N.M. Gasanly, A.F. Goncharov, B.M. Dzhavadov, N.N. Melnik, V.I. Tagirov, and E.A. Vinogradov, Phys. Status Solidi B 97 (1980) 367–377.

[44] A.G. Abdullaev, K.R. Allakhverdiev, T.D. Ibragimov, and R.M. Sardarly, Phys. Status Solidi B 128, 401 (1985).

[45] G. Orudzhev, V. Jafarova, S. Schorr, K. Mimura, K. Wakita, Y.G. Shim, N. Mamedov, and F. Hashimzade, Jap. J. Appl. Phys. 47 (2008) 8193–8199.

[46] A.V. Gomonnai, Yu.M. Vysochanskii, M.I. Gurzan, and V.Yu. Slivka, Fiz. Tverd. Tela 25 (1983) 1454–1458 [in Russian].

Figure captions

Fig. 1. Temperature profile of the two-zone crystallisation oven and the shape of the growth ampoule.

Fig. 2. $TlIn(S_{0.99}Se_{0.01})_2$ and $TlIn(S_{0.95}Se_{0.05})_2$ single crystals grown by the Bridgman technique.

Fig. 3. Powder XRD patterns for the grown $TlIn(S_{1-x}Se_x)_2$ crystals with different chemical composition. The insets show the enlarged area of the highest XRD maximum, the peak position for the $TlInS_2$ crystal being indicated by arrows.

Fig. 4. XRD patterns from the cleaved surfaces of the grown $TlIn(S_{1-x}Se_x)_2$ single crystals with different chemical composition. The insets show the enlarged area of the highest XRD maximum, the peak position for the $TlInS_2$ crystal being indicated by arrows.

Fig. 5. SEM pattern of a cleaved surface of the grown $TlIn(S_{0.94}Se_{0.06})_2$ single crystal.

Fig. 6. EDX spectra of the grown $TlIn(S_{1-x}Se_x)_2$ single crystals and the results of the elemental analysis of their chemical composition.

Fig. 7. Correlation of the EDX-based data x_{EDX} for the selenium content in the $TlIn(S_{1-x}Se_x)_2$ single crystals and the atomic fraction of Se in the initial mixture x_{mix}. The dashed straight line corresponds to the full correlation $x_{EDX} = x_{mix}$.

Fig. 8. Raman spectra of sulphur-rich $TlIn(S_{1-x}Se_x)_2$ single crystals in the Z(XX+XY)Z configuration at room temperature.

Fig. 9. Compositional dependence of the ratio of intensities of the observed bands near 200 cm^{-1} to those of sulphide-like bands slightly below 300 cm^{-1} in the Raman spectra of $TlIn(S_{1-x}Se_x)_2$ crystals.

Fig. 10. Raman spectrum of $TlInSe_2$ single crystal in the Z(XX+XY)Z configuration at room temperature.

Highlights:

– Sulphur-rich $TlIn(S_{1-x}Se_x)_2$ single crystals were grown by the Bridgman technique

– $TlIn(S_{1-x}Se_x)_2$ crystals were studied by XRD, SEM, EDX, and Raman spectroscopy

– One- and two-mode features as well as vibrations of $In_4S_{10-y}Se_y$ groups are revealed

Figure 1

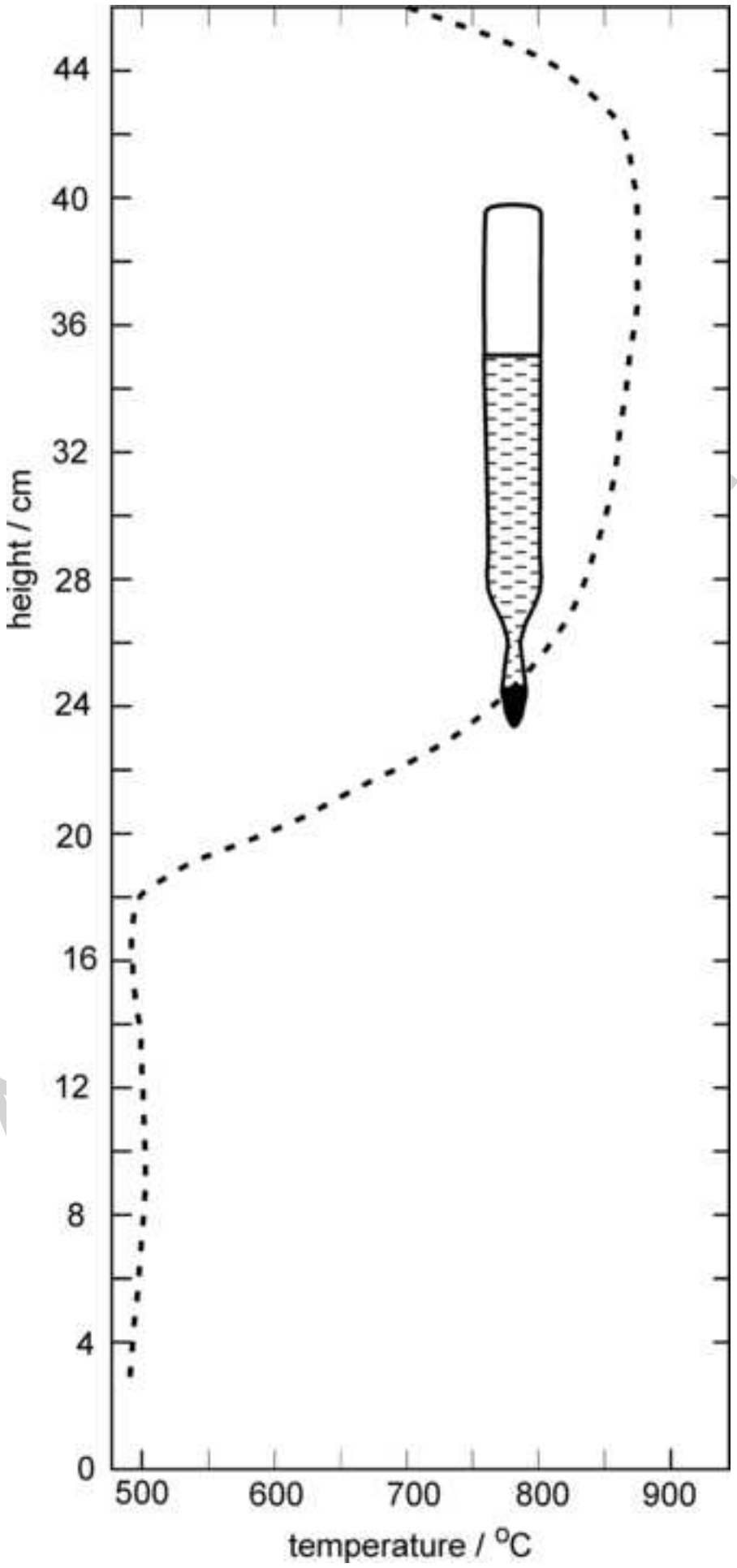

Figure 2a

Figure 2b

Figure 3

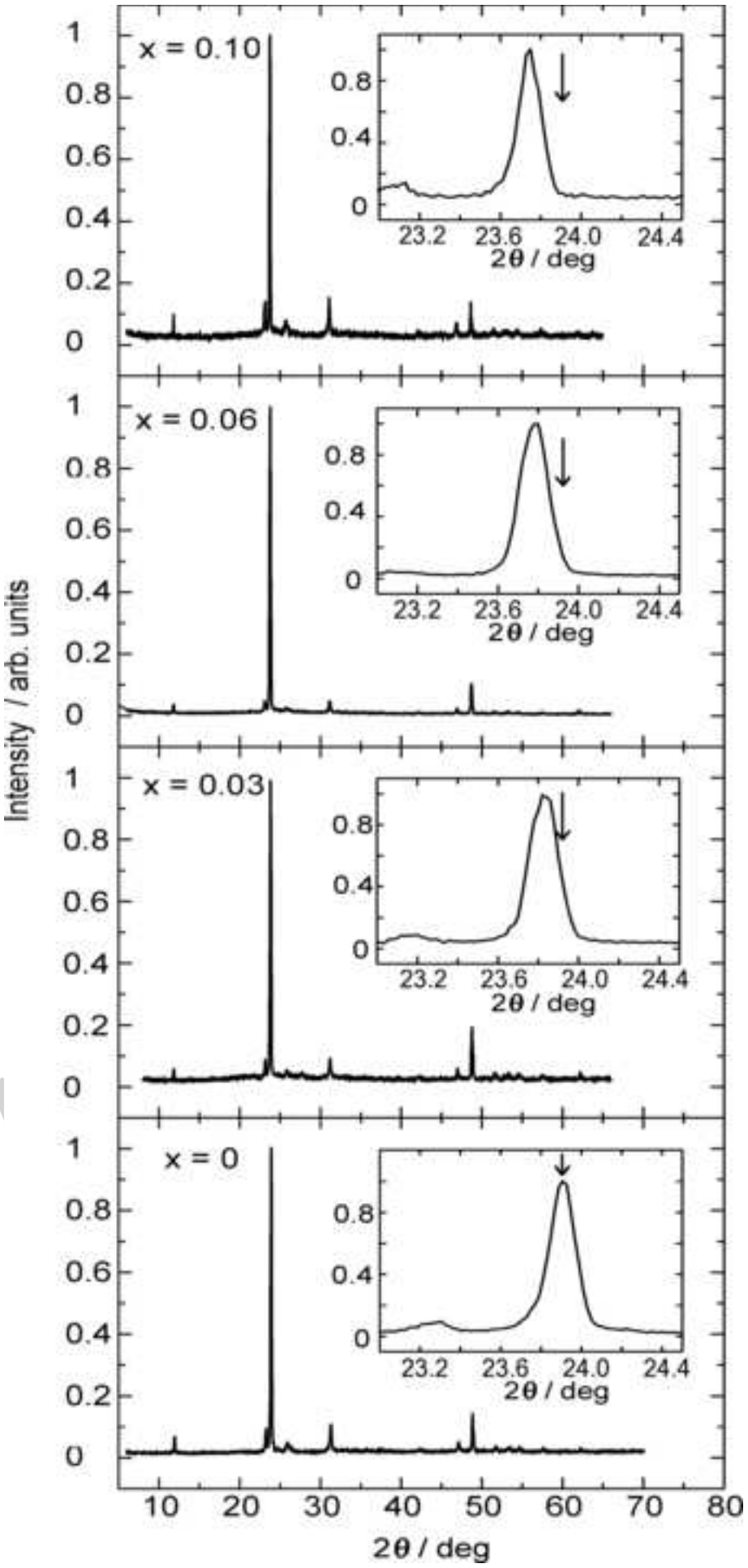

Figure 4

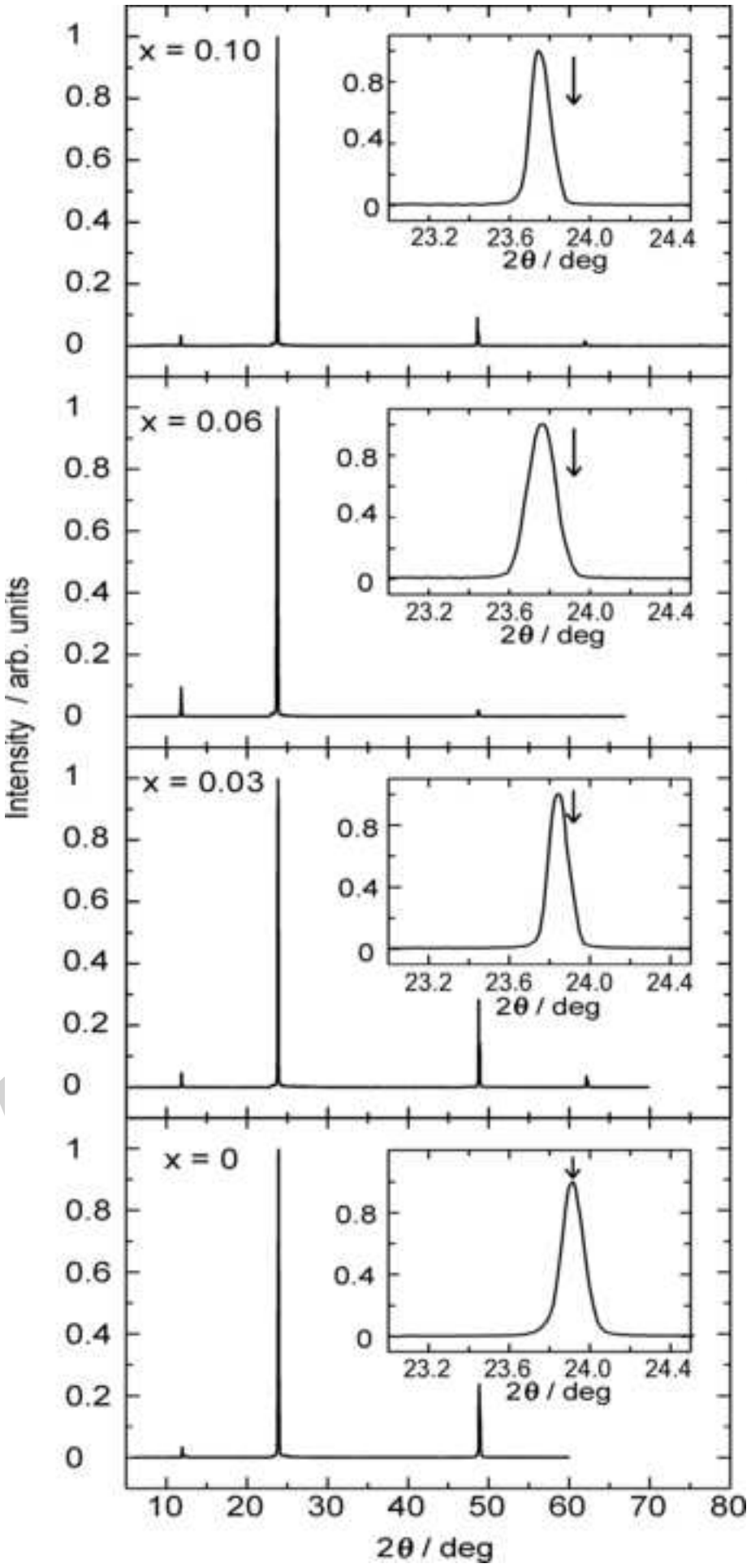

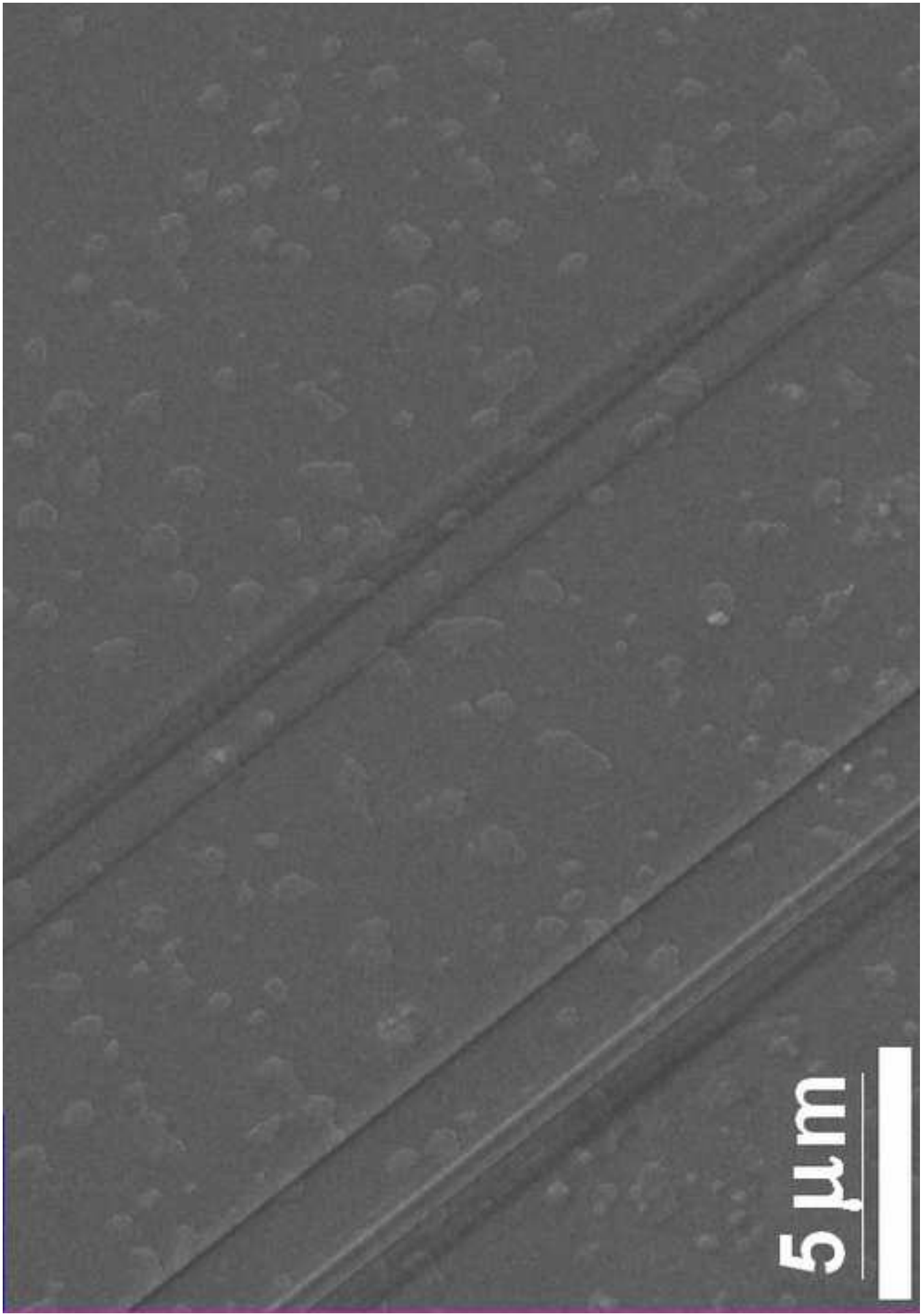

Figure 5

Figure 6

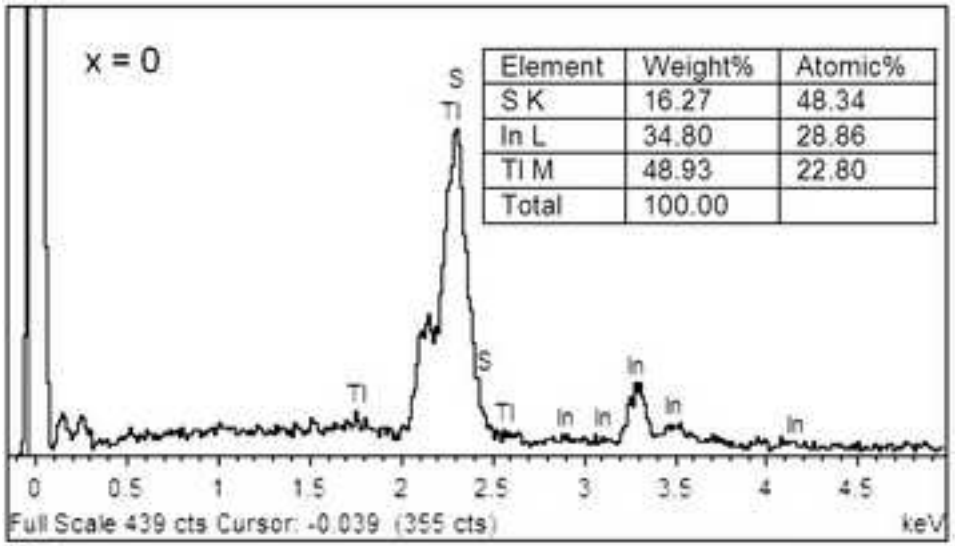

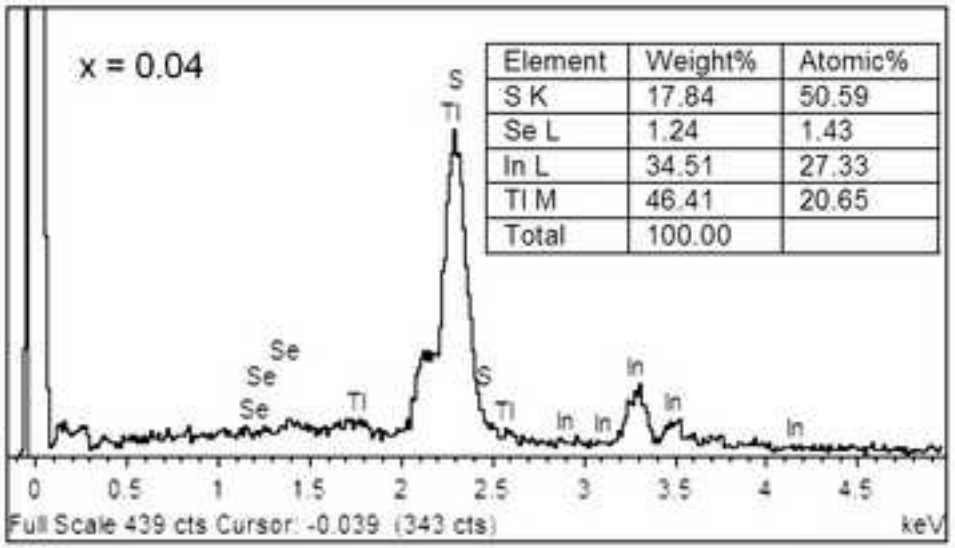

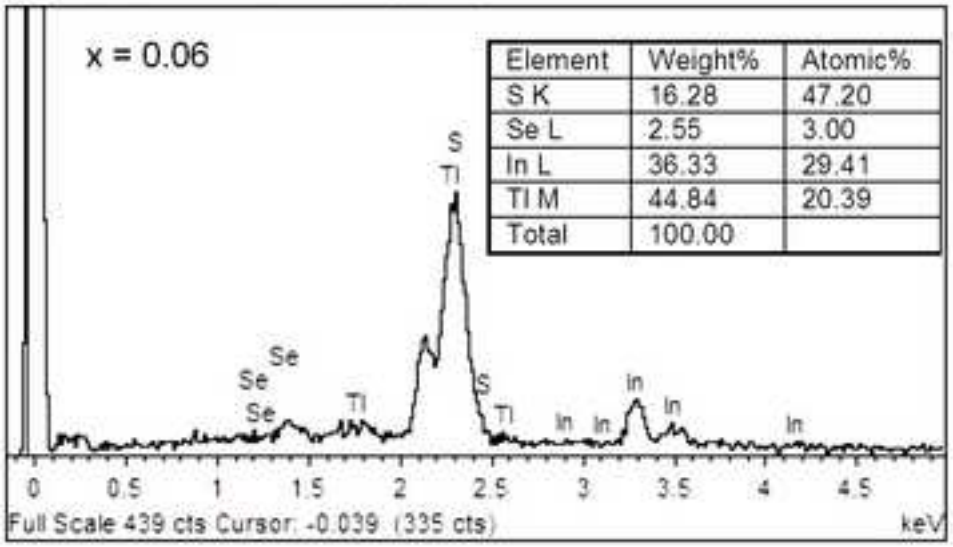

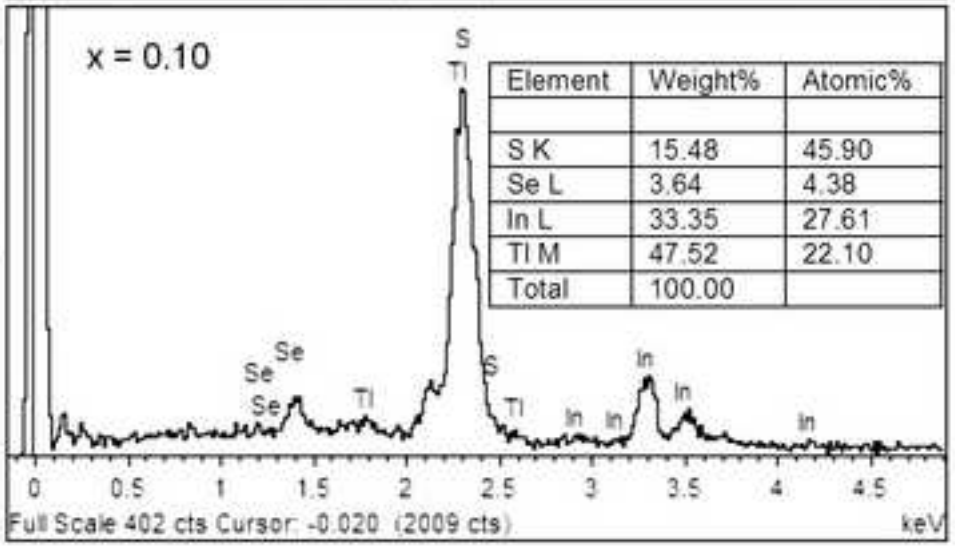

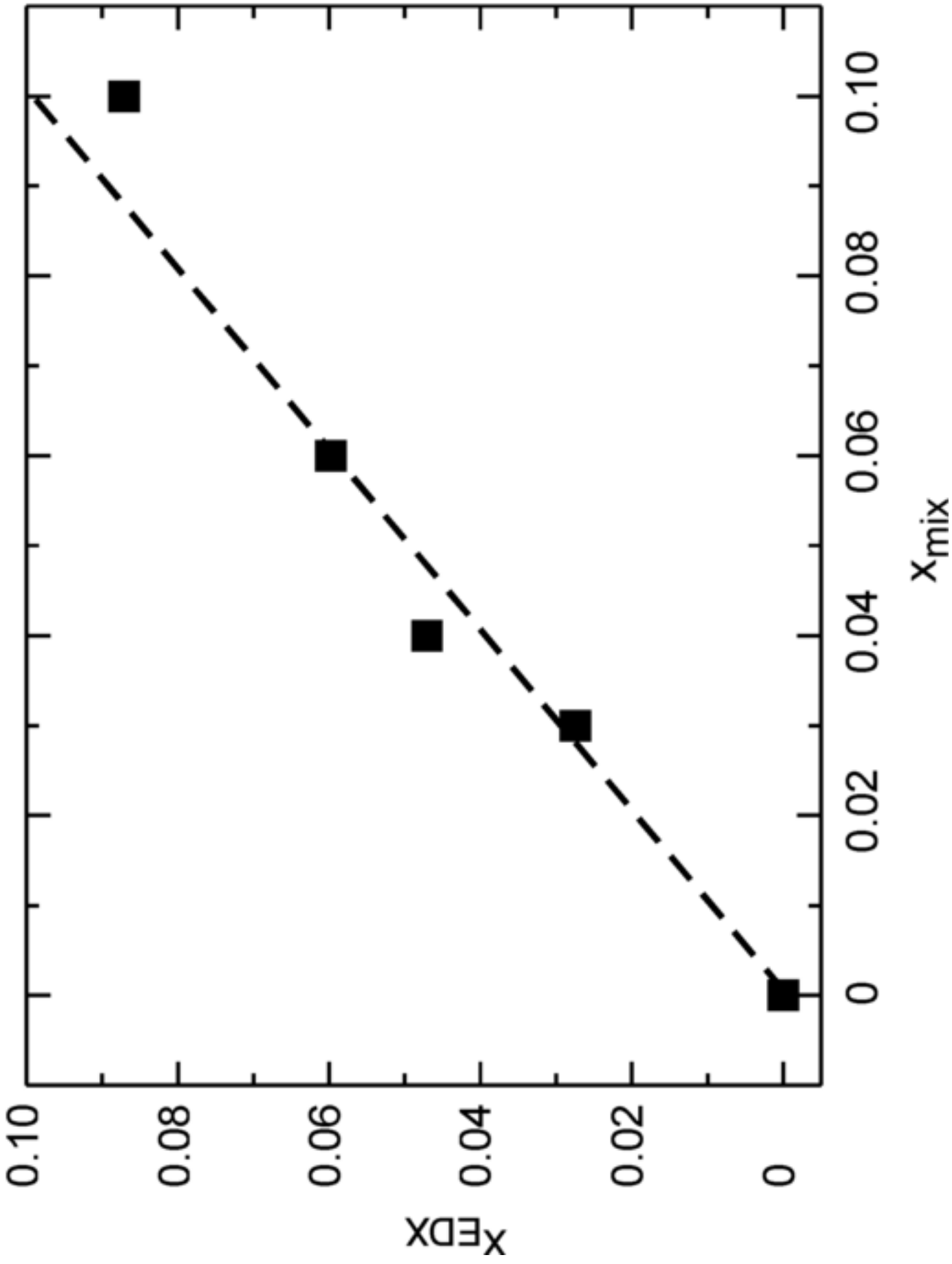

Figure 7

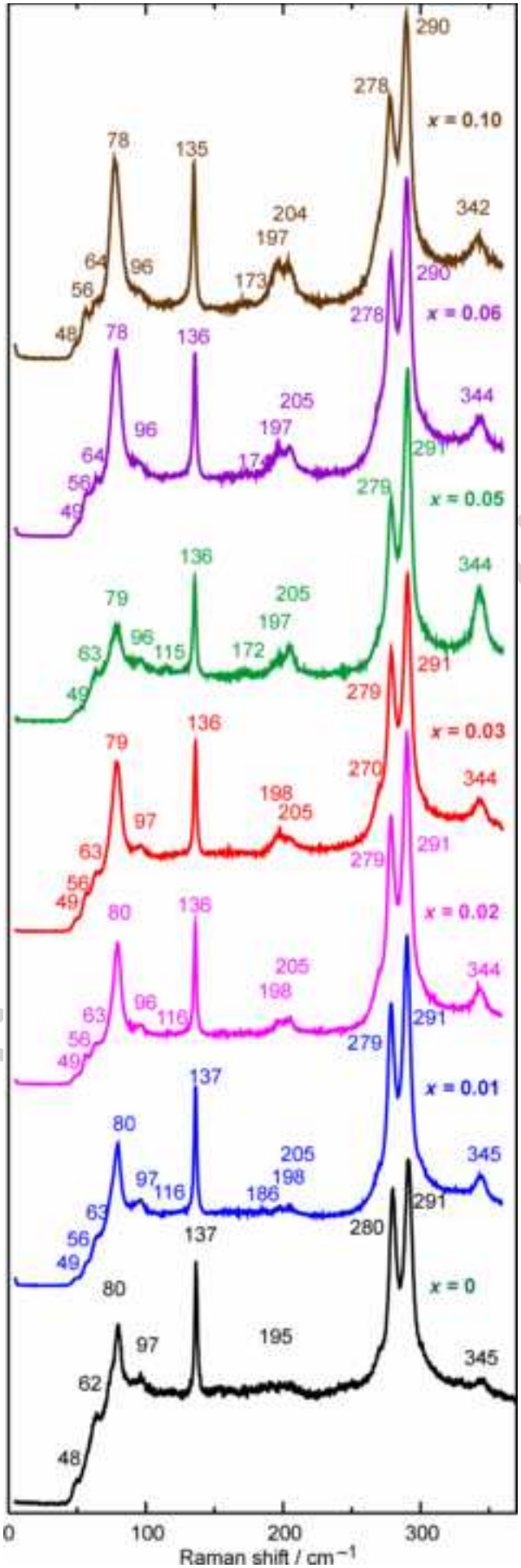

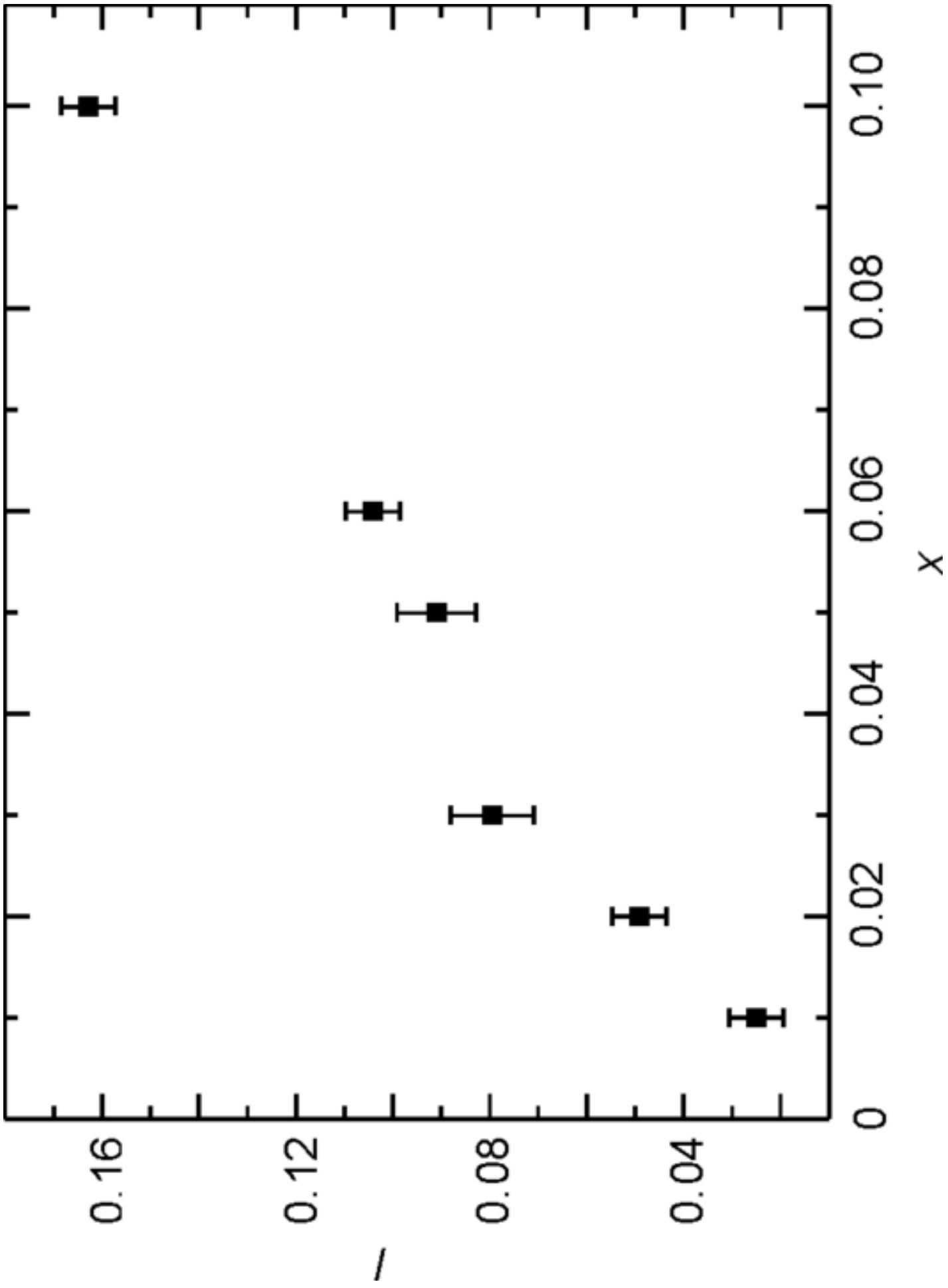

Figure 9

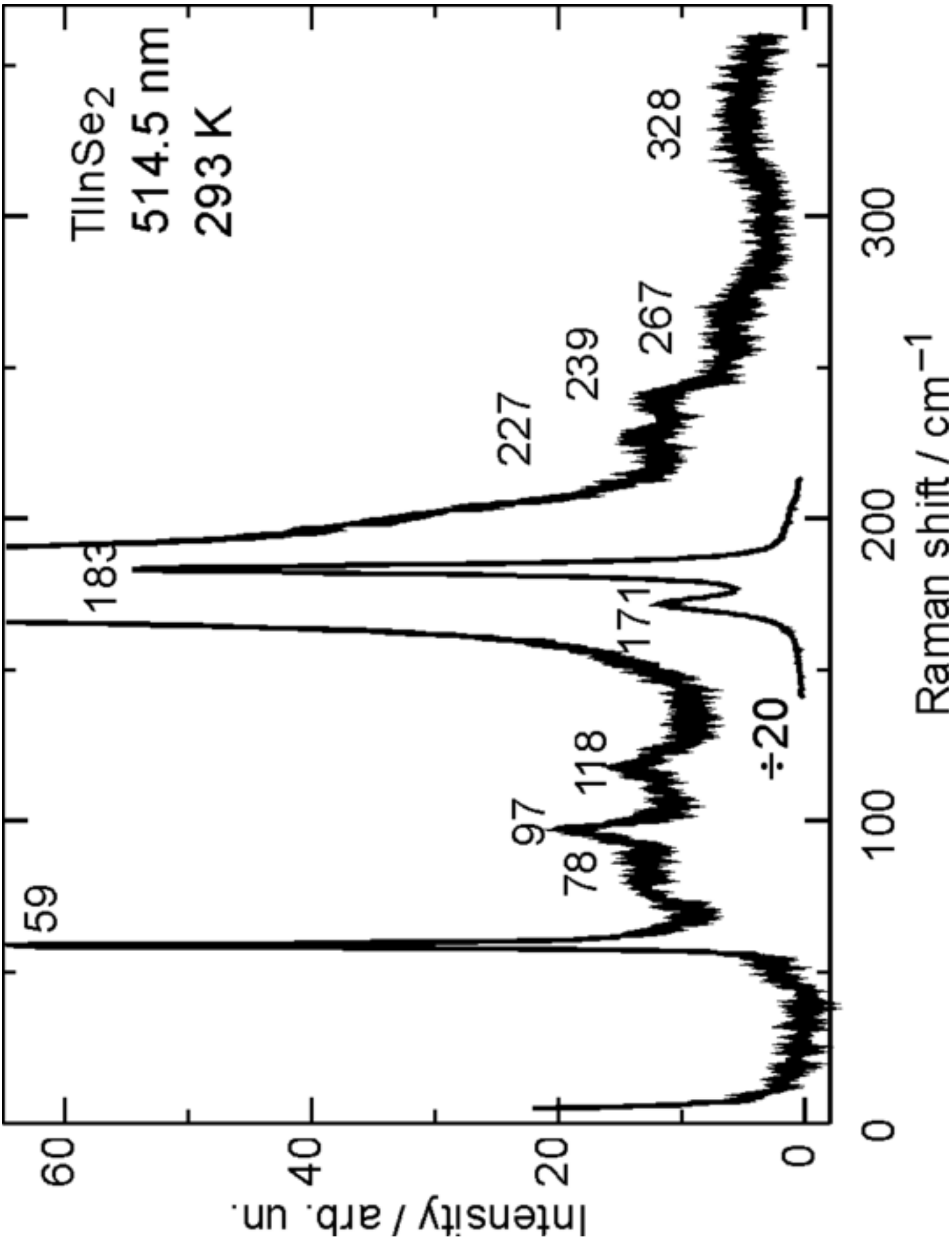
TlInSe2
514.5 nm
293 K
59
78
97
118
171
183
227
239
267
328
÷20
Intensity / arb. un.
Raman shift / cm−1
0
20
40
60
0
100
200
300

Figure 10